Indonesian Journal of Science & Technology

How to Read and Interpret FTIR Spectroscope of Organic Material

Asep Bayu Dani Nandiyanto✉, Rosi Oktiani, Risti Ragadhita

Departemen Kimia, Universitas Pendidikan Indonesia, Jl. Dr. Setiabudi no 229 Bandung 40154, Indonesia

✉Correspondence: E-mail: nandiyanto@upi.edu

ABSTRACTS

Fourier Transform Infrared (FTIR) has been developed as a tool for the simultaneous determination of organic components, including chemical bond, as well as organic content (*e.g.,* protein, carbohydrate, and lipid). However, until now, there is no further documents for describing the detailed information in the FTIR peaks. The objective of this study was to demonstrate how to read and assess chemical bond and structure of organic material in the FTIR, in which the analysis results were then compared with the literatures. The step-by-step method on how to read the FTIR data was also presented, including reviewing simple to the complex organic materials. This study is potential to be used as a standard information on how to read FTIR peaks in the biochemical and organic materials.

.

ARTICLE INFO

1. INTRODUCTION

Fourier transform infrared (FTIR) is one of the important analytical techniques for researchers. This type of analysis can be used for characterizing samples in the forms of liquids, solutions, pastes, powders, films, fibers, and gases. This analysis is also possible for analyzing material on the surfaces of substrate (Fan *et al.,* 2012). Compared to other types of characterization analysis, FTIR is quite popular. This characterization analysis is quite rapid, good in accuracy, and relatively sensitive (Jaggi and Vij, 2006).

In the FTIR analysis procedure, samples are subjected to contact with infrared (IR) radiation. The IR radiations then have impacts on the atomic vibrations of a molecule in the sample, resulting the specific absorption and/or transmission of energy. This makes the FTIR useful for determining specific molecular vibrations contained in the sample (Kirk and Othmer, 1953).

Many techniques for explaining in detail regarding the FTIR analysis have been reported (Coates, 2000; Jaggi and Vij, 2006; Kirk and Othmer, 1953). However, most papers did not report in detail about how to read and interpret the FTIR results. In fact, the way to understand in detail for beginner scientists and students are inevitable.

This report was to discuss and explain how to read and interpret FTIR data in the organic material. The analysis was then compared with the literatures. The step-by-step method on how to read the FTIR data was presented, including reviewing simple to the complex organic materials.

As a model of complex organic materials, *Lumbricus rubellus* (LR) was used. LR has quite high protein (64-76%), fat (7-10%), calcium (0.55%), phosphorus (1%), and crude fiber (1.08%) (Istiqomah *et al.,* 1958). LR also has at least 9 types of essential amino acids and 4 types of non-essential amino acids (Desi, 2016; Istiqomah *et al.,* 1958). As a consequence, LR is classified as one of the most complex organic materials. To ensure the effectiveness in the step-by-step reading procedure, various samples of LR that were heated at specific temperatures were also analyzed since LR is vulnerable against heat. We believe that this paper can be used as a basic knowledge for students and beginner scientists in comprehending and interpreting FTIR data.

2. CURRENT KNOWLEDGE FOR UNDERSTANDING FTIR SPECTRUM

2.1. Spectrum in the FTIR analysis result.

The main idea gained from the FTIR analysis is to understand what the meaning of the FTIR spectrum (see example FTIR spectrum in **Figure 1**). The spectrum can result "absorption versus wavenumber" or "transmission versus wavenumber" data. In this paper, we discuss only the "absorption versus wavenumber" curves.

In short, the IR spectrum is divided into three wavenumber regions: far-IR spectrum (<400 cm^{-1}), mid-IR spectrum (400-4000 cm^{-1}), and near-IR spectrum (4000-13000 cm^{-1}). The mid-IR spectrum is the most widely used in the sample analysis, but far- and near-IR spectrum also contribute in providing information about the samples analyzed. This study focused on the analysis of FTIR in the mid-IR spectrum.

The mid-IR spectrum is divided into four regions:

(i) the single bond region (2500-4000 cm^{-1}),

(ii) the triple bond region (2000-2500 cm^{-1}),

(iii) the double bond region (1500-2000 cm^{-1}), and

(iv) the fingerprint region (600-1500 cm^{-1}).

The schematic IR spectrum is available in **Figure 1**, and the specific frequency of each functional groups is available in **Table 1**.
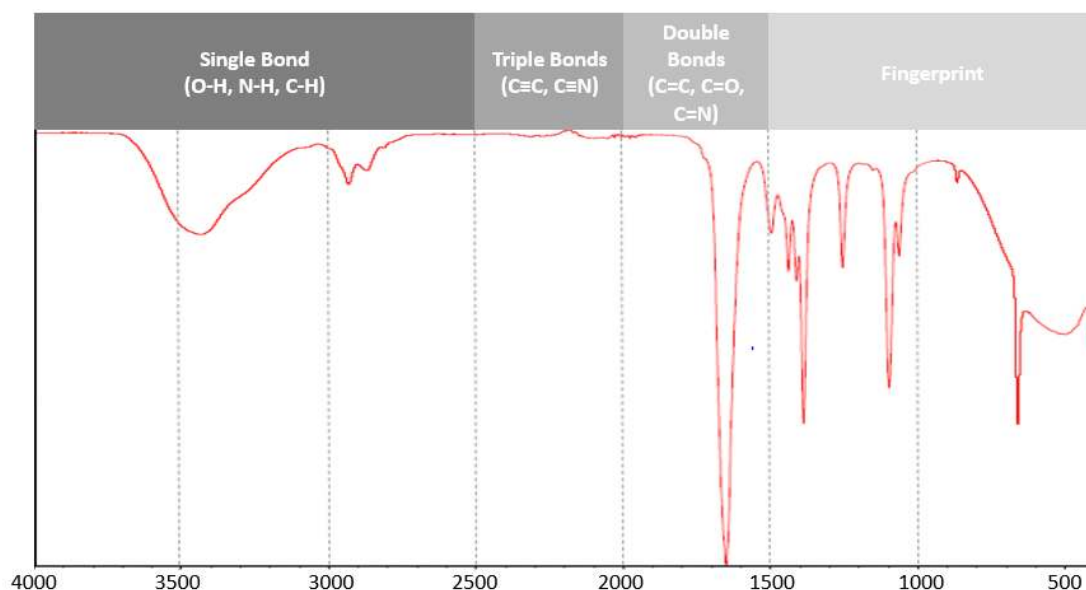
Figure 1. Mid-IR spectrum regions

Table 1. Functional group and its quantified frequencies. Data was adopted from reference (Coates, 2000)

Functional group/assignment	Wavenumber (cm^{-1})
1. Saturated Aliphatic (alkene/alkyl)	
a) Methyl (−CH$_3$)	
Methyl C-H asym./sym. Stretch	2970–2950/2880–2860
Methyl C-H asym./sym. Bend	1470–1430/1380–1370
gem-Dimethyl or ''iso''- (doublet)	1385–1380/1370–1365
Trimethyl or ''tert-butyl'' (multiplet)	1395–1385/1365
b) Methylene (>CH$_2$)	
Methylene C-H asym./sym. Stretch	2935–2915/2865–2845
Methylene C-H bend	1485–1445
Methylene —(CH$_2$)$_n$— rocking (n ≥ 3)	750–720
Cyclohexane ring vibrations	1055–1000/1005–925
c) Methyne (>CH−)	
Methyne C-H stretch	2900–2880
Methyne C-H bend	1350–1330
Skeletal C-C vibrations	1300–700
d) Special methyl (−CH$_3$) frequencies	
Methoxy, methyl ether O-CH$_3$, C-H stretch	2850–2815
Methylamino, N-CH$_3$, C-H stretch	2820–2780

Table 1 (continue). Functional group and its quantified frequencies. Data was adopted from reference (Coates, 2000)

Functional group/assignment	Wavenumber (cm⁻¹)
2. Olefinic (alkene)	
Alkenyl C=C stretch	1680–1620
Aryl-substituted C=C	1625
Conjugated C=C	1600
Terminal (vinyl) C-H stretch	3095–3075
	3040–3010
Pendant (vinylidene) C-H stretch	3095–3075
Medial, cis- or trans-C-H stretch	3040–3010

Table 1 (continue). Functional group and its quantified frequencies. Data was adopted from reference (Coates, 2000)

Functional group/assignment	Wavenumber (cm⁻¹)
Vinyl C-H in-plane bend	1420–1410
Vinylidene C-H in-plane bend	1310–1290
Vinyl C-H out-of-plane bend	995–985 + 915–890
Vinylidene C-H out-of-plane bend	895–885
trans-C-H out-of-plane bend	970–960
cis-C-H out-of-plane bend	700 (broad)
3. Olefinic (alkene)	
Alkenyl C=C stretch	1680–1620
Aryl-substituted C=C	1625
Conjugated C=C	1600
Terminal (vinyl) C-H stretch	3095–3075
	3040–3010
Pendant (vinylidene) C-H stretch	3095–3075
Medial, cis- or trans-C-H stretch	3040–3010
Vinyl C-H in-plane bend	1420–1410
Vinylidene C-H in-plane bend	1310–1290
Vinyl C-H out-of-plane bend	995–985 + 915–890
Vinylidene C-H out-of-plane bend	895–885
trans-C-H out-of-plane bend	970–960
cis-C-H out-of-plane bend	700 (broad)
4. Aromatic ring (aryl)	
C=C-C Aromatic ring stretch	1615–1580
	1510–1450
Aromatic C-H stretch	3130–3070
Aromatic C-H in-plane bend	1225–950 (several)
Aromatic C-H out-of-plane bend	900–670 (several)
C-H Monosubstitution (phenyl)	770–730 + 710–690
C-H 1,2-Disubstitution (ortho)	770–735
C-H 1,3-Disubstitution (meta)	810–750 + 900–860
C-H 1,4-Disubstitution (para)	860–800
Aromatic combination bands	2000–1660 (several)

Table 1 (continue). Functional group and its quantified frequencies. Data
was adopted from reference (Coates, 2000)

Functional group/assignment	Wavenumber (cm^{-1})
5. Acetylenic(alkyne)	
C≡C Terminal alkyne (monosubstituted)	2140–2100
C≡C Medial alkyne (disubstituted)	2260–2190
Alkyne C-H stretch	3320–3310
Alkyne C-H bend	680–610
Alkyne C-H bend	630 (typical)
6. Aliphatic organohalogen compound	
Aliphatic fluoro compounds, C-F stretch	1150–1000
Aliphatic chloro compounds, C-Cl stretch	800–700
Aliphatic bromo compounds, C-Br stretch	700–600
Aliphatic iodo compounds, C-I stretch	600–500
7. Alcohol and hydroxy compound	
Hydroxy group, H-bonded OH stretch	3570–3200 (broad)
Normal ''polymeric'' OH stretch	3400–3200
Dimeric OH stretch	3550–3450
Internally bonded OH stretch	3570–3540
Nonbonded hydroxy group, OH stretch	3645–3600 (narrow)
Primary alcohol, OH stretch	3645–3630
Secondary alcohol, OH stretch	3635–3620
Tertiary alcohol, OH stretch	3620–3540
Phenols, OH stretch	3640–3530
Primary or secondary, OH in-plane bend	1350–1260
Phenol or tertiary alcohol, OH bend	1410–1310
Alcohol, OH out-of-plane bend	720–590
Primary alcohol, C-O stretch	~1050
Secondary alcohol, C-O stretch	~1100
Tertiary alcohol, C-O stretch	~1150
Phenol, C-O stretch	~1200
8. Ether and oxy compound	
Methoxy, C-H stretch (CH$_3$-O-)	2820–2810
Alkyl-substituted ether, C-O stretch	1150–1050
Cyclic ethers, large rings, C-O stretch	1140–1070
Aromatic ethers, aryl -O stretch	1270–1230
Epoxy and oxirane rings	~1250 + 890–800[1]
Peroxides, C-O-O- stretch	890–820[1]

Table 1 (continue). Functional group and its quantified frequencies. Data was adopted from reference (Coates, 2000)

Functional group/assignment	Wavenumber (cm^{-1})
9. Ether and oxy compound	
Methoxy, C-H stretch (CH$_3$-O-)	2820–2810
Alkyl-substituted ether, C-O stretch	1150–1050
Cyclic ethers, large rings, C-O stretch	1140–1070
Aromatic ethers, aryl -O stretch	1270–1230
Epoxy and oxirane rings	~1250 + 890–800[1]
Peroxides, C-O-O- stretch	890–820[1]
a) Primary amino	
Aliphatic primary amine, NH stretch	3400–3380 + 3345–3325
Aromatic primary amine, NH stretch	3510–3460 + 3415–3380
Primary amine, NH bend	1650–1590
Primary amine, CN stretch	1090–1020
b) Secondary amino	
Aliphatic secondary amine, >N-H stretch	3360–3310
Aromatic secondary amine, >N-H stretch	~3450
Heterocyclic amine, >N-H stretch	3490–3430
Imino compounds, =N-H stretch	3350–3320
Secondary amine, >N-H bend	1650–1550
Secondary amine, CN stretch	1190–1130
c) Tertiary amino	
Tertiary amine, CN stretch	1210–1150
d) Aromatic amino	
Aromatic primary amine, CN stretch	1340–1250
Aromatic secondary amine, CN stretch	1350–1280
Aromatic tertiary amine, CN stretch	1360–1310
10. Carbonyl compound	
Carboxylate (carboxylic acid salt)	1610–1550/1420–1300
Amide	1680–1630
Quinone or conjugated ketone	1690–1675/(1650–1600)[2]
Carboxylic acid	1725–1700
Ketone	1725–1705
Aldehyde	1740–1725/(2800–2700)[3]
Ester	1750–1725
Six-membered ring lactone	1735
Alkyl carbonate	1760–1740
Acid (acyl) halide	1815–1770
Aryl carbonate	1820–1775
Five-membered ring anhydride	1870–1820/1800–1775
Transition metal carbonyls	2100–1800

Table 1 (continue). Functional group and its quantified frequencies. Data was adopted from reference (Coates, 2000)

Functional group/assignment	Wavenumber (cm^{-1})
11. Nitrogen multiple and cumulated double bond compound	
Aliphatic cyanide/nitrile	2280–2240
Aromatic cyanide/nitrile	2240–2220
Cyanate (-OCN and C-OCN stretch)	2260–2240/1190–1080
Isocyanate (-N=C=O asym. stretch)	2276–2240
Thiocyanate (-SCN)	2175–2140
Isothiocyanate (-NCS)	2150–1990
Open-chain imino (-C=N-)	1690–1590
Open-chain azo (-N=N-)	1630–1575
12. Simple hetero-oxy compounds	
a) Nitrogen-oxy compounds	
Aliphatic nitro compounds	1560–1540/1380–1350[4]
Organic nitrates	1640–1620/1285–1270[4]
Aromatic nitro compounds	1555–1485/1355–1320[4]
b) Phosphorus-oxy compounds	
Organic phosphates (P=O stretch)	1350–1250
Aliphatic phosphates (P-O-C stretch)	1050–990
Aromatic phosphates (P-O-C stretch)	1240–1190/995–850
c) Sulfur-oxy compounds	
Dialkyl/aryl sulfones	1335–1300/1170–1135[4]
Organic sulfates	1420–1370/1200–1180[4]
Sulfonates	1365–1340/1200–1100[4]
d) Silicon-oxy compounds	
Organic siloxane or silicone (Si-O-Si)	1095–1075/1055–1020
Organic siloxane or silicone (Si-O-C)	1110–1080
13. Thiols and thio-substituted compounds	
Thiols (S-H stretch)	2600–2550
Thiol or thioether, CH2-S-(C-S stretch)	710–685
Thioethers, CH$_3$-S-(C-S stretch)	660–630
Aryl thioethers, ø-S (C-S stretch)	715–670
Disulfides (C-S stretch)	705–570
Disulfides (S-S stretch)	620–600
Aryl disulfides (S-S stretch)	500–430
Polysulfides (S-S stretch)	500–470
14. Common inorganic ions	
Carbonate ion	1490–1410/880–860[5]
Sulfate ion	1130–1080/680–610[5]
Nitrate ion	1380–1350/840–815[5]
Phosphate ion	1100–1000
Ammonium ion	3300–3030/1430–1390[5]
Cyanide ion, thiocyanate ion, and related ions	2200–2000
Silicate ion	1100–900

Note: 1) Normally, it is very weak in the infrared but more characteristic in the Raman spectrum; 2)Lower frequency band because of the conjugated double bond; 3)Higher frequency band characteristic of aldehydes, related with the terminal aldehydic C-H stretch; 4)Asymmetric/symmetric XO2 stretch (NO2 and SO2); 5)Normally, the first absorption is intense and broad, and the second has weak to medium intensity and narrow. The both often exist as multiple band structures, and it may be used to characterize individual compounds.

2.2. Step-by-step Analysis Procedure.

There are five steps to interpret FTIR:

1. **Step 1:** Identification of number of absorption bands in the entire IR spectrum. If the sample has a simple spectrum (has less than 5 absorption bands, the compounds analyzed are simple organic compounds, small mass molecular weight, or inorganic compounds (such as simple salts). But, if the FTIR spectrum has more than 5 absorption bands, the sample can be a complex molecule.

2. **Step 2:** Identifying single bond area (2500-4000 cm^{-1}). There are several peaks in this area:
   (1) A broad absorption band in the range of between 3650 and 3250 cm^{-1}, indicating hydrogen bond. This band confirms the existence of hydrate (H2O), hydroxyl (-OH), ammonium, or amino. For hydroxyl compound, it should be followed by the presence of spectra at frequencies of 1600–1300, 1200–1000 and 800–600 cm^{-1}. However, if there is a sharp intensity absorption in the absorption areas of 3670 and 3550 cm^{-1}, it allows the compound to contain an oxygen-related group, such as alcohol or phenol (illustrates the absence of hydrogen bonding).
   (2) A narrow band at above 3000 cm^{-1}, indicating unsaturated compounds or aromatic rings. For example, the presence of absorption in the wavenumber of between 3010 and 3040 cm^{-1} confirms the existence of simple unsaturated olefinic compounds.
   (3) A narrow band at below 3000 cm^{-1}, showing aliphatic compounds. For example, absorption band for long-chain linear aliphatic compounds is identified at 2935 and 2860 cm^{-1}. The

bond will be followed by peaks at between 1470 and 720 cm^{-1}.
   (4) Specific peak for Aldehyde at between 2700 and 2800 cm^{-1}.

3. **Step 3:** Identifying the triple bond region (2000-2500 cm^{-1})
   For example, if there is a peak at 2200 cm^{-1}, it should be absorption band of C≡C. The peak is usually followed by the presence of additional spectra at frequencies of 1600–1300, 1200–1000 and 800–600 cm^{-1}.

4. **Step 4**: Identifying the double bond region (1500-2000 cm^{-1})
   Double bound can be as carbonyl (C = C), imino (C = N), and azo (N = N) groups.
   (1) 1850 - 1650 cm^{-1} for carbonyl compounds
   (2) Above 1775 cm^{-1}, informing active carbonyl groups such as anhydrides, halide acids, or halogenated carbonyl, or ring-carbonyl carbons, such as lactone, or organics carbonate.
   (3) Range of between 1750 and 1700 cm^{-1}, describing simple carbonyl compounds such as ketones, aldehydes, esters, or carboxyl.
   (4) Below 1700 cm^{-1}, replying amides or carboxylates functional group.
   (5) If there is a conjugation with another carbonyl group, the peak intensities for double bond or aromatic compound will be reduced. Therefore, the presence of conjugated functional groups such as aldehydes, ketones, esters, and carboxylic acids can reduce the frequency of carbonyl absorption.
   (6) 1670 - 1620 cm^{-1} for unsaturation bond (double and triple bond). Specifically, the peak at 1650 cm^{-1} is for double bond carbon or olefinic compounds (C = C). Typical conjugations with other double bond structures such as C = C, C = O or

aromatic rings will reduce the intensity frequency with intense or strong absorption bands. When diagnosing unsaturated bonds, it is also necessary to check absorption below 3000 cm^{-1}. If the absorption band is identified at 3085 and 3025 cm^{-1}, it is intended for C-H. Normally C-H has absorption above 3000 cm^{-1}.

(7) Strong intensity at between 1650 and 1600 cm^{-1}, informing double bonds or aromatic compounds.

(8) Between 1615 and 1495 cm^{-1}, responding aromatic rings. They appeared as two sets of absorption bands around 1600 and 1500 cm^{-1}. These aromatic rings usually followed by the existence of weak to moderate absorption in the area of between 3150 and 3000 cm^{-1}(for C-H stretching).

For the simple aromatic compounds, several bands can be also observed between 2000 and 1700 cm^{-1}in the form of multiple bands with a weak intensity. It is also support the aromatic ring absorption band (at 1600/1500 cm^{-1}absorption frequency), namely C-H bending vibration with the intensity of medium absorption to strong which sometimes has single or multiple absorption bands found in the area between 850 and 670 cm^{-1}.

5. **Step 5**: Identifying the fingerprint region (600-1500 cm^{-1})

This area is typically specific and unique. See detailed information in **Table 1**. But, several identification can be found:

(1) Between 1000 and 880 cm^{-1} for multiple band absorption, there are absorption bands at 1650, 3010, and 3040 cm^{-1}.

(2) For C-H (out-of-plane bending), it should be combined with absorption bands at 1650, 3010, and 3040 cm^{-1}

which show characteristics of compound unsaturation.

(3) Regarding vinyl-related compound, about 900 and 990 cm^{-1} for identifing vinyl terminals (-CH=CH$_2$), between 965 and 960 cm^{-1} for trans unsatrated vinyl (CH=CH), and about 890 cm^{-1} for double olefinic bonds in single vinyl (C=CH$_2$).

(4) Regarding aromatic compound, a single and strong absorption band is around 750 cm^{-1} for orto and 830 cm^{-1} for para.

3. EXPERIMENTAL METHOD

To understand how to read and interpret the FTIR analysis, the present study used several FTIR patterns. Two FTIR patterns were obtained from reference (Coates, 2000) (as a standard comparison) and the others are from LR microparticles.

In short of the experimental procedure for the preparation of LR microparticles, LR was obtained and purchased from CV Bengkel dan Agrobisnis, Indonesia. Prior to using, LR was washed in warm water (temperature of 40°C) for several hours. The washed LR was then dried at 70°C for about 15 minutes in the electrical drier. The dried LR was then put into a batch-typed saw-milling apparatus, in which the saw-milling process was explained in our previous study (Nandiyanto *et al.,* 2018a). Then, for evaluating the formation of carbon particles from LR, 0.360 g of saw-milled LR was put into an electrical furnace and heated in the atmospheric condition under a fixed condition: a heating rate of 50°C/min and a holding time at a specific temperature for 30 min. To obtain the clear evaluation in the transformation of LR into carbon particles, heating temperatures were varied from 80 to 250°C in a small step of almost every 10°C. The heated material was subsequently cooled to room temperature with a cooling rate of 50°C/min. To support the FTIR

analysis, FTIR (FTIR-4600, Jasco Corp., Japan) was utilized.

4. RESULTS AND DISCUSSION
4.1. FTIR analysis of sample gained from literature

Figure 2 shows the analysis of 2-propanone. To understand the appearance peaks in the FTIR below, step-by-step process can be used. The results can be concluded as follows:

(1) Regarding the number of peaks, there are more than five peaks, informing that the analyzed chemical is not a simple chemical.

(2) The peaks contained single bond area (2500-4000 cm^{-1}).
   - No broad absorption band was found, informing there is no hydrogen bond in the material.
   - There is a sharp bond at about 3500 cm^{-1}, replying the existence of oxygen-related bonding.
   - No other peaks between 3000 and 3200 cm^{-1} was found, informing there is no aromatic structure
   - Narrow bond at less than 3000 cm^{-1} responded to the C-C bond.
   - No specific peak for aldehyde has been found at between 2700 and 2800 cm^{-1}.

(3) No triple bond region (2000-2500 cm^{-1}) was detected, informing no C≡C bond in the material.

(4) Regarding the double bond region (1500-2000 cm^{-1}), there is a huge and sharp peak was detected at about 1700 cm^{-1}. This informs some carbonyl double bond, which can be from ketones, aldehydes, esters, or carboxyl. Since there is no specific peak for aldehyde at between 2700 and 2800 cm^{-1} (as desribed in the previous step), the prospective peak for carbonyl should be from ketone. No peak at about 1600 cm^{-1}, informing there is no C=C bonding in the material.

(5) Based on above interpretation, several conclusions can be obtained, including the analyzed material has no hydrate component. This material has ketones-related component, no double or triple bond in the material. Since the peaks were only about 10 peaks, the material should be a small organic compound.

(6) The other example in the FTIR analysis is shown in **Figure 3**. This figure is the FTIR analysis result of toluene
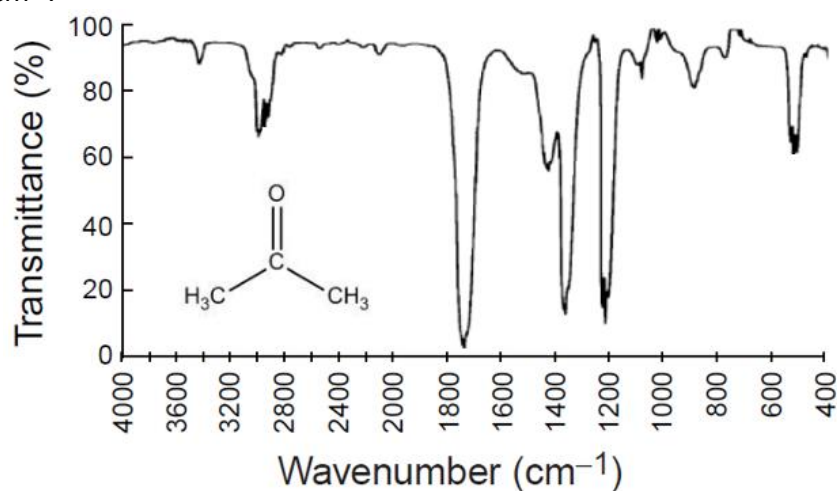

Figure 2. Example of FTIR spectra 1. Adopted from: Coates (2000)

(7) The result showed that a lot of numbers of peaks were detected, informing the complex structure material

(8) In the single bond area (2500-4000 cm^{-1}), several peaks were detected.
   - No broad absorption band in the range of between 3650 and 3250 cm^{-1}, indicating no hydrogen bond.
   - Peaks at between 3000 and 3200 cm^{-1}, replying the aromatic ring.
   - Peaks at below 3000 cm^{-1}, responding the single bond of carbon.
   - No aldehyde peak was detected at between 2700 and 2800 cm^{-1}.

(9) Regarding the triple bond region (2000-2500 cm^{-1}), no peak was detected, informing no C≡C bonding.

(10) In the double bond region (1500-2000 cm^{-1}), several peaks were detected:
   - Above 1775 cm^{-1}, informing active carbonyl groups, in which this should be from ring-carbonyl carbons.
   - Range of between 1750 and 1700 cm^{-1}, describing simple carbonyl compounds, in which this is due to the bonding between methyl (CH3) to the benzene ring.
   - Huge band at about 1600 cm^{-1}, informing double bonds or aromatic compounds.

(11) In the fingerprint region (600-1500 cm^{1}), strong signal was found at about 1500 cm^{-1} (informing aromatic ring). Vinyl-related compound was also found at about 1000 cm^{-1}.

Based on the above analysis, the analysis showed that the material has aromatic ring, and simple functional bonding (methyl). This is in a good agreement with the chemical compound of toluene.

4.2. FTIR analysis of the LR microparticles

FTIR analysis results of saw-milled LR particles are shown in **Figure 4**. This figure shows the change of FTIR peak and pattern. There is a change in the peaks after the heating process. Informing there is a change in the chemical structure. In short, since LR is vulnerable against heat, this should be the decomposition of organic component into carbon material. The change in the FTIR peak and pattern was found when heating at temperature that higher than 180 ℃, in which the FTIR pattern was near to the carbon as explained in the literature (Nandiyanto *et al.,* 2016, Nandiyanto *et al.,* 2017).

Using above interpreting method and compared to the literature for some organic material, ftir peaks are shown in **Table 2**. The results shows that these peaks contained several organic materials. This can be used as a standard ftir peaks for organic materials, related to protein, carbohydrate, fat, etc.
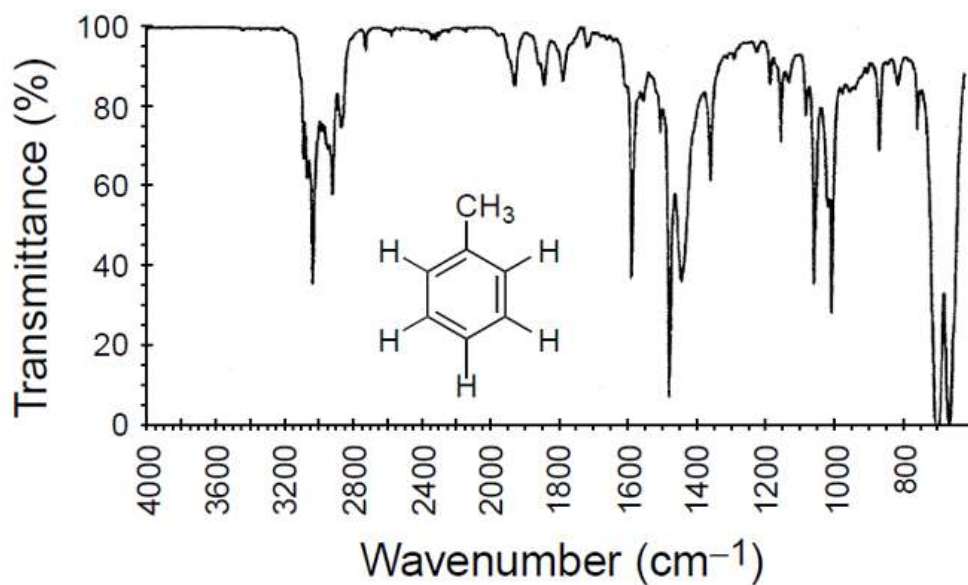
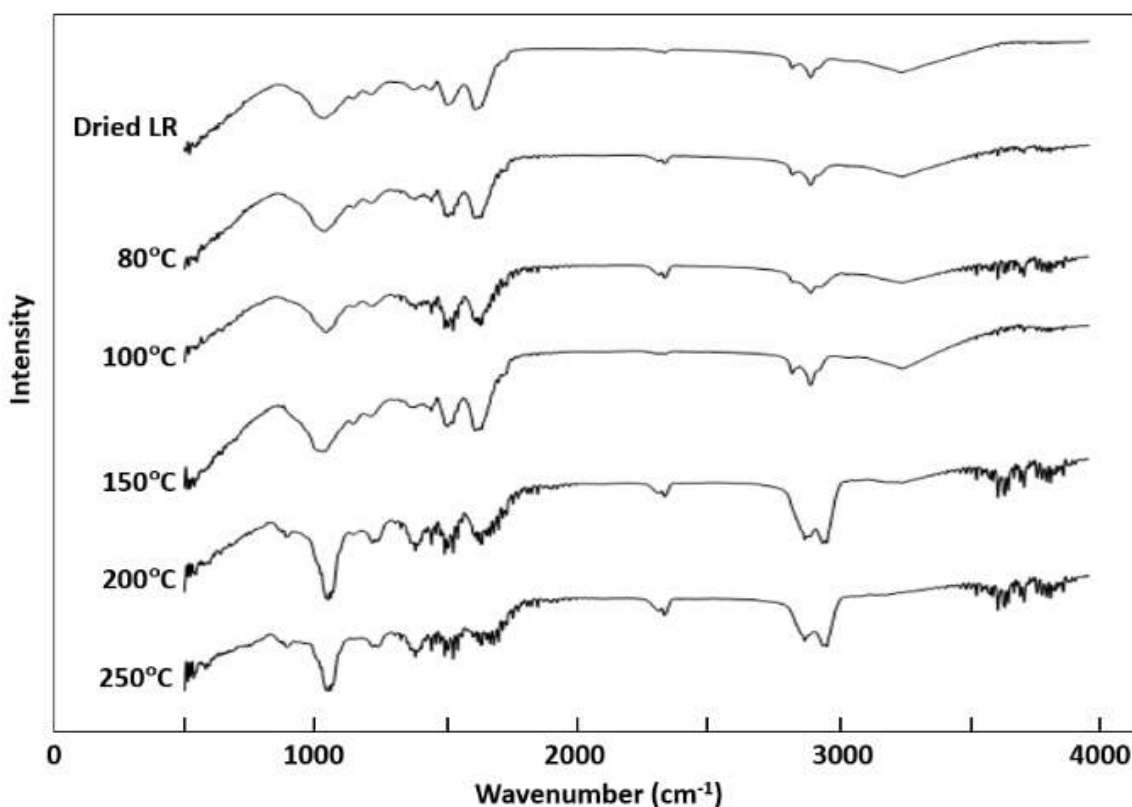**Figure 3.** Example of FTIR spectra 2. Adopted from: Coates (2000)

Figure 4. FTIR analysis results of saw-milled LR heated with various temperatures

Table 2. FTIR peaks identified in LR

No	Wavenumber		Assignment	Possible nutrient type	Ref.
	Exp.	Lit.			
1	601	600-608	CH out-of-plane bending vibrations	Organic material	(Chiang *et al.*, 1999)
2	929**	about 930	Ring deformation of phenyl carbon-related component	Carbon	(Schulz and Baranska, 2007) (Nandiyanto *et al.*, 2016, Nandiyanto *et al.*, 2017)
3	1051	1045-1053	Gives an estimate carbohydrate concentrations (lower in malignant cells) C-O-O-C C-O stretching coupled with C-O bending of the C-OH of carbohydrates Glycogen C-O-C stretching (nucleic acids and phospholipids), C-O-C stretching of DNA and RNA Indicates a degree of oxidative damage to DNA Phosphate, oligosaccharides, PO2- stretching modes, P-O-C antisymmetric stretching mode of phosphate ester, and C-OH stretching of oligosaccharides Phosphate I band for two different C-O vibrations of deoxyribose in DNA in A and B forms of helix or ordering structure C-O in carbohydrates	Carbohydrate	(Huleihel *et al.*, 2002, Mordechai *et al.*, 2001) (Paluszkiewicz and Kwiatek, 2001) (Wang *et al.*, 1997) (Wood *et al.*, 1998) (Fabian *et al.*, 1995) (Andrus and Strickland, 1998) (Yoshida *et al.*, 1997) (Dovbeshko *et al.*, 2002) (Fung *et al.*, 1996)

Table 2 (continue). FTIR peaks identified in LR

No	Wavenumber		Assignment	Possible nutrient type	Ref.
	Exp.	Lit.			
4	1160	1159-1164	C-O of proteins and carbohydrates, stretching modes of the C-OH groups of serine, threonine, and tyrosine residues of cellular proteins, hydrogen-bonded stretching mode of C-OH groups	Protein (serine, threosine, and tyrosine) and collagen	(Fung *et al.*, 1996)
			CO stretching, stretching vibrations of hydrogen-bonding C-OH groups		(Wang *et al.*, 1997)
			Mainly from the C-O stretching mode of C-OH groups of serine, threosine, and tyrosine of proteins		(Fujioka *et al.*, 2004)
			C-C, C-OH, C-O stretching		(Wong *et al.*, 1993, Yang *et al.*, 2005)
			C-O-C, ring (polysaccharides, cellulose)		(Shetty *et al.*, 2006)
			CH deformations		(Schulz and Baranska, 2007)
			C-O stretching band of collagen (type I)		(Fukuyama *et al.*, 1999)
			Mainly from the C-O stretching mode of C-OH groups of serine, threosine, and tyrosine of proteins		(Yang *et al.*, 2005)
			n(CC), d(COH), n(CO) stretching		(Lucassen *et al.*, 1998, Yang *et al.*, 2005)
			C-O stretching (in normal tissue)		(Rigas *et al.*, 1990)

Table 2 (continue). FTIR peaks identified in LR

No	Wavenumber		Assignment	Possible nutrient type	Ref.
	Exp.	Lit.			
5	1233	1230-1238		Protein (Amide III)	(Chiriboga *et al.*, 1998, Dovbeshko *et al.*, 2002)
			Stretching PO2- asymmetric		
			Overlapping of the protein amide III and the nucleic acid phosphate vibration, composed of amide III as well as phosphate vibration of nucleic acids, amide III		(Chiriboga *et al.*, 1998)
			C-H component		(Schulz and Baranska, 2007)
			Amide III and asymmetric phosphodiester stretching mode (PO2-), mainly from the nucleic acids		(Eckel *et al.*, 2001)
			PO2- of nucleic acids		(Fung *et al.*, 1996)
			Relatively specific for collagen and nucleic acids		(Andrus and Strickland, 1998)
			Stretching PO2⁻ asymmetric (phosphate I), PO2- asymmetric (phosphate I), Stretching PO2- asymmetric (phosphate I)		(Dovbeshko *et al.*, 2000)
			PO2- asymmetric		(Barry *et al.*, 1992)
			Asymmetric phosphate [PO2- (asym.)] stretching modes		(Wang *et al.*, 1997)
			Stretching PO2- asymmetric		(Dovbeshko *et al.*, 2002)
			Asymmetric PO2- stretching		(Fukuyama *et al.*, 1999)

Table 2 (continue). FTIR peaks identified in LR

No	Wavenumber		Assignment	Possible nutrient type	Ref.
	Exp.	Lit.			
6	1401	1400-1403	Symmetric stretching vibration of COO- group of fatty acids and amino acids	Protein and Collagen	(Wood *et al.*, 1996)
			CH₃ of proteins, symmetric bending modes of methyl groups in skeletal proteins, CH₃ of collagen		(Fung *et al.*, 1996)
			Specific absorption of proteins		(Argov *et al.*, 2004)
			Symmetric stretch of methyl groups in protein		(Fujioka *et al.*, 2004, Wood *et al.*, 1998)
			Ring stretching vibrations mixed strongly with CH in-plane bending		(Schulz and Baranska, 2007)
			COO₂ symmetric stretching of acidic amino acids aspartate and glutamate, and fatty acids		(Fabian *et al.*, 1995)
			CH₃ symmetric deformation		(Agarwal *et al.*, 2006)
			Symmetric CH₃ bending modes of the methyl groups of proteins		(Fujioka *et al.*, 2004)
					(Barry *et al.*, 1992, Fujioka *et al.*, 2004, Lucassen *et al.*, 1998, Rigas and Wong, 1992, Wu *et al.*, 2001)
			(CH₃) symmetric Stretching C-N, deformation N-H, deformation C-H		(Dovbeshko *et al.*, 2000)
			C(CH₃)₂ symmetric		(Yang *et al.*, 2005)
7	1410**	about 1410	Carbon-related component	carbon	(Nandiyanto *et al.*, 2016, Nandiyanto *et al.*, 2017)

Table 2 (continue). FTIR peaks identified in LR

No	Wavenumber		Assignment	Possible nutrient type	Ref.
	Exp.	Lit.			
8	1457	1455-1458	C-O-H Less characteristic, due to aliphatic side groups of the amino acid residues CH$_3$ of proteins, symmetric bending modes of methyl groups in skeletal proteins, CH$_3$ of collagen	Protein and Collagen	(Dovbeshko *et al.,* 2000) (Chiriboga *et al.,* 1998) (Fung *et al.,* 1996)
			Asymmetric CH$_3$ bending modes of the methyl groups of proteins		(Fujioka *et al.,* 2004)
			(CH$_3$) asymmetric		(Fujioka *et al.,* 2004, Lucassen *et al.,* 1998, Wong *et al.,* 1991, Yang *et al.,* 2005)
			CH$_3$ bending vibration (lipids and proteins)		(Fabian *et al.,* 1995)
			Extremely weak peaks of DNA & RNA arises mainly from the vibrational modes of methyl and methylene groups of proteins and lipids and amide groups		(Wang *et al.,* 1997)
			Asymmetric CH$_3$bending modes of the methyl groups of proteins		(Fujioka *et al.,* 2004)
9	1522	1517-1526	Amide II	Protein (Amide II)	(Paluszkiewicz and Kwiatek, 2001)
			Stretching C=N, C=C, C=N guanine		(Dovbeshko *et al.,* 2000)
10	1633	1630-1635	Amide I	Protein (Amide I)	(Wood *et al.,* 1998)
			C-C stretch of phenyl		(Schulz and Baranska, 2007) (Dovbeshko *et al.,* 2000)
			C=C uracyl, C=O Amide I		(Eckel *et al.,* 2001)

Table 2 (continue). FTIR peaks identified in LR

No	Wavenumber		Assignment	Possible nutrient type	Ref.
	Exp.	Lit.			
11	1651	1649-1652	Unordered random coils and turns of amide I	Protein (Amide I)	(Eckel *et al.*, 2001)
			C=O, C=N, N-H of adenine, thymine, guanine, cytosine		(Dovbeshko *et al.*, 2002)
			O-H bending (water) Amide I absorption (predominantly the C=O stretching vibration of the amide C=O)		(Fabian *et al.*, 1995) (Wood *et al.*, 1996, Wood *et al.*, 1998)
			Protein amide I absorption, C2=O cytosine		(Dovbeshko *et al.*, 2000)
			C=O, stretching C=C uracyl, NH2 guanine Peptide amide I		(Andrus, 2006, Sukuta and Bruch, 1999)
			Amide I		(Mordechai *et al.*, 2004)
12	1747	1745-1750	Ester group (C=O) vibration of triglycerides	Fat	(Wu *et al.*, 2001)
			C=O, polysaccharides, pectin, C=C, lipids, fatty Acid		(Shetty *et al.*, 2006)
13	2332	about 2350	NH component	Amino-related component	(Nandiyanto *et al.*, 2018b)
14	2341	about 2350	NH component	Amino-related component	(Nandiyanto *et al.*, 2018b)
15	2359	about 2350	NH component	Amino-related component	(Nandiyanto *et al.*, 2018b)
16	2857*	2853-2860	CH2 of lipids, Asymmetric CH2 stretching mode of the methylene chains in membrane lipids	Fat	(Fung *et al.*, 1996)
			Stretching C-H		(Dovbeshko *et al.*, 2000)
17	2925	2923-2930	C-H stretching bands in malignant and normal tissues	Fat	(Wu *et al.*, 2001)
			Stretching C-H		(Dovbeshko *et al.*, 2000)
			CH$_2$ lipids		(Fung *et al.*, 1996)
			CH$_2$		(Yang *et al.*, 2005)
18	2958**	2956-2959	Asymmetric stretching vibration of CH$_3$ of acyl chains (lipids)	Fat	(Fabian *et al.*, 1995)
			C-H stretching		(Wu *et al.*, 2001)
			CH$_3$ of lipids, DNA, and proteins, asymmetric stretching mode of the methyl groups from cellular proteins, nucleic acids, and lipids		(Fung *et al.*, 1996)

Table 2 (continue). FTIR peaks identified in LR

No	Wavenumber		Assignment	Possible nutrient type	Ref.
	Exp.	Lit.			
19	2991**	about 3000		Carbon	(Nandiyanto *et al.*, 2016, Nandiyanto *et al.*, 2017)
			Carbon-related component		
20	3092	3078-3111		Organic material	(Dovbeshko *et al.*, 2000)
			C-H ring		
21	3284**	3273-3293		Water	(Dovbeshko *et al.*, 2000, Schulz and Baranska, 2007)
			Stretching O-H symmetric		

Note: * appeared in the initial raw LR; ** appeared after heating LR with temperature of more than 180℃

5. CONCLUSION

The present study demonstrated the simplest ways for understanding FTIR analysis results. The step-by-step method on how to read the FTIR data was presented in detail, including reviewing simple to the complex organic materials. This study also tested to the analysis of LR microparticles since this material has quite complicated organic structure. To ensure the effectiveness in the step-by-step reading procedure, various samples of LR that were heated at specific temperatures were also analyzed, since LR is vulnerable against heat. We believe that this paper can be used as a basic knowledge for students and beginner scientists in comprehending and interpreting FTIR data.

6. ACKNOWLEDGEMENTS

7. AUTHORS' NOTE

The author(s) declare(s) that there is no conflict of interest regarding the publication of this article. Authors confirmed that the data and the paper are free of plagiaris.

8. REFERENCES

Agarwal, R., Tandon, P., and Gupta, V. D. (2006). Phonon dispersion in poly (dimethylsilane). *Journal of Organometallic Chemistry*, 691(13), 2902-2908.

Andrus, P. G., and Strickland, R. D. (1998). Cancer grading by Fourier transform infrared spectroscopy. *Biospectroscopy*, 4(1), 37-46.

Andrus, P. G. (2006). Cancer monitoring by FTIR spectroscopy. *Technology in cancer research and treatment*, 5(2), 157-167.

Argov, S., Sahu, R. K., Bernshtain, E., Salman, A., Shohat, G., Zelig, U., and Mordechai, S. (2004). Inflamatory bowel diseases as an intermediate stage between normal and cancer: A FTIR-microspectroscopy approach. *Biopolymers: Original Research on Biomolecules*, 75(5), 384-392.

Barry, B. W., Edwards, H. G. M., and Williams, A. C. (1992). Fourier transform Raman and infrared vibrational study of human skin: assignment of spectral bands. *Journal of Raman spectroscopy*, 23(11), 641-645.

Chiang, H. P., Song, R., Mou, B., Li, K., Chiang, P., Wang, D., Tse, W., and Ho, L. (1999). Fourier transform Raman spectroscopy of carcinogenic polycyclic aromatic hydrocarbons in biological systems: Binding to heme proteins. *Journal of Raman spectroscopy*, 30(7), 551-555.

Chiriboga, L., Xie, P., Yee, H., Vigorita, V., Zarou, D., Zakim, D., and Diem, M. (1998). Infrared spectroscopy of human tissue. I. Differentiation and maturation of epithelial cells in the human cervix. *Biospectroscopy*, 4(1), 47-53.

Coates, J. (2000). Interpretation of infrared spectra, a practical approach. *Encyclopedia of analytical chemistry*, 12, 10815-10837.

Desi, I. R. (2016). *Isolasi dan Karakterisasi Senyawa Alkaloid dari Cacing Tanah (Lumbricus Rubellus Hoffmeister)* (Doctoral dissertation, Fakultas MIPA (UNISBA)).

Dovbeshko, G., Chegel, V., Gridina, N. Y., Repnytska, O., Shirshov, Y., Tryndiak, V., Todor, I., and Solyanik, G. (2002). Surface enhanced IR absorption of nucleic acids from tumor cells: FTIR reflectance study. *Biopolymers: Original Research on Biomolecules*, 67(6), 470-486.

Dovbeshko, G. I., Gridina, N. Y., Kruglova, E. B., and Pashchuk, O. P. (2000). FTIR spectroscopy studies of nucleic acid damage. *Talanta*, 53(1), 233-246.

Eckel, R., Huo, H., Guan, H. W., Hu, X., Che, X., and Huang, W. D. (2001). Characteristic infrared spectroscopic patterns in the protein bands of human breast cancer tissue. *Vibrational Spectroscopy*, 27(2), 165-173.

Fabian, H., Jackson, M., Murphy, L., Watson, P. H., Fichtner, I., and Mantsch, H. H. (1995). A comparative infrared spectroscopic study of human breast tumors and breast tumor cell xenografts. *Biospectroscopy*, 1(1), 37-45.

Fan, M., Dai, D., and Huang, B. (2012). Fourier transform infrared spectroscopy for natural fibres. *In Fourier transform-materials analysis: InTech*.

Fujioka, N., Morimoto, Y., Arai, T., and Kikuchi, M. (2004). Discrimination between normal and malignant human gastric tissues by Fourier transform infrared spectroscopy. *Cancer Detection and Prevention*, 28(1), 32-36.

Fukuyama, Y., Yoshida, S., Yanagisawa, S., and Shimizu, M. (1999). A study on the differences between oral squamous cell carcinomas and normal oral mucosas measured by Fourier transform infrared spectroscopy. *Biospectroscopy*, 5(2), 117-126.

Fung, M. F. K., Senterman, M. K., Mikhael, N. Z., Lacelle, S., and Wong, P. T. (1996). Pressure-tuning fourier transform infrared spectroscopic study of carcinogenesis in human endometrium. *Biospectroscopy*, 2(3), 155-165.

Huleihel, M., Salman, A., Erukhimovitch, V., Ramesh, J., Hammody, Z., and Mordechai, S. (2002). Novel spectral method for the study of viral carcinogenesis in vitro. *Journal of biochemical and biophysical methods*, 50, 111-121.

Istiqomah, L., Sofyan, A., Damayanti, E., and Julendra, H. (2009). Amino acid 7. profile of earthworm and earthworm meal (Lumbricus rubellus) for animal feedstuff. *Journal of the Indonesian Tropical Animal Agriculture*, 34(4), 253-257.

Moore S, Spackman D. H, and Stein W. H. (1958). Chromatography of amino 8. acids on sulfonated polystyrene resins. *An improved system. Anal Chem*, 30(7), 1185-1190.

Jaggi, N., and Vij, D. (2006). Fourier transform infrared spectroscopy. In Handbook of Applied Solid State Spectroscopy. Boston: Springer, 411-450.

Kirk, R. E., and Othmer, D. F. (1953). Encyclopedia of Chemical Technology Vol. 2. *The Interscience Encyclopedia*, Inc; New York.

Lucassen, G. W., Van Veen, G. N., and Jansen, J. A. (1998). Band analysis of hydrated human skin stratum corneum attenuated total reflectance Fourier transform infrared spectra in vivo. *Journal of biomedical optics*, 3(3), 267-281.

Mordechai, S., Mordehai, J., Ramesh, J., Levi, C., Huleihal, M., Erukhimovitch, V., Moser, A., and Kapelushnik, J. (2001). Application of FTIR microspectroscopy for the follow-up of childhood leukemia chemotherapy. *Subsurface and Surface Sensing Technologies and Applications*, 3, 243-251.

Mordechai, S., Sahu, R. K., Hammody, Z., Mark, S., Kantarovich, K., Guterman, H., Podshyvalov, J., Goldstein, J., and Argov, S. (2004). Possible common biomarkers from FTIR microspectroscopy of cervical cancer and melanoma. *Journal of Microscopy*, 215(1), 86-41.

Nandiyanto, A. B. D., Fadhlulloh, M. A., Rahman, T., and Mudzakir, A. (2016). Synthesis of carbon nanoparticles from commercially available liquified petroleum gas. *IOP Conference Series: Materials Science and Engineering*, 128(1), 012042.

Nandiyanto, A. B. D., Putra, Z. A., Andika, R., Bilad, M. R., Kurniawan, T., Zulhijah, R., and Hamidah, I. (2017). Porous activated carbon particles from rice straw waste and their adsorption properties. *Journal of Engineering Science and Technology*, 12, 1-11.

Nandiyanto, A. B. D., Andika, R., Aziz, M., and Riza, L. S. (2018a). Working Volume and Milling Time on the Product Size/Morphology, Product Yield, and Electricity Consumption in the Ball-Milling Process of Organic Material. *Indonesian Journal of Science and Technology*, 3(2), 82-94.

Nandiyanto, A. B. D., Oktiani, R., Ragadhita, R., Sukmafitri, A., and Zaen, R. (2018b). Amorphous content on the photocatalytic performance of micrometer-sized tungsten trioxide particles. *Arabian Journal of Chemistry*, in press.

Paluszkiewicz, C., and Kwiatek, W. M. (2001). Analysis of human cancer prostate tissues using FTIR microspectroscopy and SRIXE techniques. *Journal of Molecular Structure*, 565, 329-334.

Rigas, B., Morgello, S., Goldman, I. S., and Wong, P. T. (1990). Human colorectal cancers display abnormal Fourier-transform infrared spectra. *Proceedings of the National Academy of Sciences*, 87(20), 8140-8144.

Rigas, B., and Wong, P. T. (1992). Human colon adenocarcinoma cell lines display infrared spectroscopic features of malignant colon tissues. *Cancer Research*, 52(1), 84-88.

Schulz, H., and Baranska, M. (2007). Identification and quantification of valuable plant substances by IR and Raman spectroscopy. *Vibrational Spectroscopy*, 43(1), 13-25.

Shetty, G., Kendall, C., Shepherd, N., Stone, N., and Barr, H. (2006). Raman spectroscopy: elucidation of biochemical changes in carcinogenesis of oesophagus. *British journal of cancer*, 94(10), 1460-1464.

Sukuta, S., and Bruch, R. (1999). Factor analysis of cancer fourier transform infrared evanescent wave fiberoptical (FTIR-FEW) spectra. *Lasers in Surgery and Medicine*, 24(5), 382-388.

Wang, H., Wang, H. C., and Huang, Y. J. (1997). Microscopic FTIR studies of lung cancer cells in pleural fluid. *Science of the Total Environment*, 204(3), 283-287.

Wong, P. T., Goldstein, S. M., Grekin, R. C., Godwin, T. A., Pivik, C., and Rigas, B. (1993). Distinct infrared spectroscopic patterns of human basal cell carcinoma of the skin. *Cancer Research*, 53(4), 762-765.

Wong, P. T. T., Papavassiliou, E. D., and Rigas, B. (1991). Phosphodiester stretching bands in the infrared spectra of human tissues and cultured cells. *Applied spectroscopy*, 45(9), 1563-1567.

Wood, B. R., Quinn, M. A., Burden, F. R., and McNaughton, D. (1996). An investigation into FTIR spectroscopy as a biodiagnostic tool for cervical cancer. *Biospectroscopy*, 2(3), 143-153.

Wood, B. R., Quinn, M. A., Tait, B., Ashdown, M., Hislop, T., Romeo, M., and McNaughton, D. (1998). FTIR microspectroscopic study of cell types and potential confounding variables in screening for cervical malignancies. *Biospectroscopy*, 4(2), 75-91.

Wu, J. G., Xu, Y. Z., Sun, C. W., Soloway, R. D., Xu, D. F., Wu, Q. G., and Xu, G. X. (2001). Distinguishing malignant from normal oral tissues using FTIR fiber-optic techniques. *Biopolymers: Original Research on Biomolecules*, 62(4), 185-192.

Yang, Y., Sulé-Suso, J., Sockalingum, G. D., Kegelaer, G., Manfait, M., and El Haj, A. J. (2005). Study of tumor cell invasion by Fourier transform infrared microspectroscopy. *Biopolymers: Original Research on Biomolecules*, 78(6), 311-317.

Yoshida, S., Miyazaki, M., Sakai, K., Takeshita, M., Yuasa, S., Sato, A., Kobayashi, T., Watanabe, S., and Okuyama, H. (1997). Fourier transform infrared spectroscopic analysis of rat brain microsomal membranes modified by dietary fatty acids: possible correlation with altered learning behavior. *Biospectroscopy*, 3(4), 281-290.